Studies on drug resistance and biofilm formation in *Candida glabrata*: focus on the implementation and optimization of CRISPR-Cas9 tools for *C. glabrata* genome editing

Inês Malpique [1,2]

Supervisors: Miguel Teixeira[1,2], Pedro Pais[1,2]

[1] Bioengineering Department (DBE), Instituto Superior Técnico, Universidade de Lisboa, Portugal

[2] Institute for Bioengineering and Biosciences (iBB), Lisbon, Portugal

ABSTRACT

Invasive fungal infections are estimated to kill around 1.5 million people every year. Although *C. albicans* is found to be the leading cause of invasive candidiasis, the emergence of *Candida glabrata* as a particularly antifungal resistant human pathogen attracted the attention of researchers, with concerns about health issues. In this dissertation, the known mechanisms of *C. glabrata* pathogenicity, including drug resistance, biofilm formation and host-pathogen interactions are reviewed. Specifically, among several genes associated with the acquisition of antifungal resistance and biofilm formation in *C. glabrata*, the role of the Rpn4, Mar1, Efg1 and Tec1 transcription factors is addressed. The first part of this work consists of a proof-of-concept, where several protocols were tested in order to implement and optimize a one vector CRISPR-Cas9 system for gene deletion in the *C. glabrata* KCHr606_Δ*ura3* strain. Following optimization, this system was successfully used to delete *RPN4* and *EFG1*, aiming their functional characterization to uncover a potential role in azole resistance and biofilm formation, respectively. Unfortunately, due to the current COVID-19 pandemics, no susceptibility and biofilm quantification assays of the mutants were accomplished, neither was the generation of CRISPR-Cas9-mediated *Cg*Δ*mar1* and *Cg*Δ*tec1* single deletion mutants and other planned multiple deletion mutants. Considering the role of Mar1, the two "GGGGAGG" motifs found in the *RSB1* promoter, which have been previously identified as potential Mar1 binding sites, were mutated through site-directed mutagenesis, and shown to influence *RSB1* gene expression in the presence of fluconazole. An upcoming Chromatin Immunoprecipitation (ChIP) analysis of the binding between Mar1 and the given motifs from *RSB1* promoter will be necessary to confirm the hypothesis of Mar1 being involved in fluconazole-induced stress responses in *C. glabrata* through the direct regulation of *RSB1*. Overall, this work describes the implementation and optimization of CRISPR technology in *C. glabrata* and provides biological material that will prove useful in deciphering the role of new players in antifungal drug resistance and biofilm formation in this pathogen.

INTRODUCTION

It is estimated that invasive fungal infections can kill around 1.5 million people every year[1]. With an increase in the number of individuals sensitive to invasive fungal infections, it is seen that the leading cause of opportunistic mycoses worldwide is *Candida* species[2,3]. Different studies have shown that *C. glabrata* is now the second or third most isolated species from patients with Invasive Candidiasis in the USA and Europe[4–6]. Although *C. glabrata* also colonises the oral cavity, vagina, and gut of healthy humans as innocuous commensals, it is especially recurrent in immunocompromised individuals as is the case of cancer patients, the elderly and patients receiving intensive care[4,7–9]. Moreover, it is the main species exhibiting multiazole, echinocandin and multidrug resistance[9]. This propensity for diseased host colonisation and higher drug resistance is possibly the answer to why the overall mortality seen with *C. glabrata* is so high (30-70%) when compared to other *Candida* species (15-40%)[7,10,11]. Generally, it is hard to obtain an accurate and fast diagnosis of Candidiasis as it is usually diagnosed late and only considered after antibiotic treatments fail. Besides, there are only four main classes of antifungals being currently used - azoles, polyenes, echinocandins and pyrimidine analogs[12,13] -, a limitation that lowers the probability of the treatment being successful and even increases the probability of a fatal outcome when the pathogen displays multidrug resistance (MDR)[12]. Several risk factors have been identified for *C. glabrata* bloodstream infections, the most common being previous fluconazole use and prior exposure to a broad spectrum of antibiotics, the use of indwelling devices like urinary or venal catheters, and surgery (such as organ transplantation)[6,7,9–11,14,15].

Biofilms are the most prevalent type of microbial growth in nature and confer substantial protection and resistance to antifungal therapy, which results in persistent infections. *Candida* cells detached from biofilms seem to have a higher association with mortality than equivalent planktonic cells[16]. Indeed, mortality was found to be higher in patients infected by isolates that formed biofilms when compared to infections by non-biofilm-forming isolates[17,18]. It has been demonstrated that *C. albicans* Δ*efg1* strains exhibit markedly altered biofilm phenotypes compared to wildtype strains. Moreover, different studies identified Efg1[19] as a regulator of *TEC1* expression, a gene that encodes a transcription factor (TF) known to modulate hyphal development in *C. albicans* as well. Among several *C. glabrata* TFs identified in our lab as biofilm regulators, *CgEFG1* and *CgTEC1* were found to have a considerable impact on biofilm formation (Cavalheiro *et al*, unpublished results). Thus, it seems relevant to further study the role of *EFG1* and *TEC1* in *C. glabrata* virulence. Additionally, a possible link between the *RPN4* gene and azole resistance in *C. glabrata* was recently uncovered in our lab[20], and very recently Mar1 was also found to confer azole drug resistance in this pathogen (Pais *et al*, unpublished results). Hence, further studies are ongoing to understand the mechanisms underlying Rpn4 and Mar1-dependent antifungal resistance of *C. glabrata*.

Given the need to apply genome engineering tools to study the molecular basis of pathogen features, the CRISPR-Cas9 system has become very popular as it is simple to design, inexpensive and extremely versatile for a variety of biological applications and cell types/organisms. This system allows the editing of an organism's genome in an efficient target-specific manner. By selecting a gene of interest, one can construct a correspondent guide RNA that will direct a nuclease (Cas) protein to the target sequence of the genome and create a double-strand break in the DNA. The development of the CRISPR-Cas9 system revealed to be a great asset for genome engineering and was soon adapted to *C. glabrata*.

This work aimed to contribute to the functional characterization of four genes with suspected important roles in *C. glabrata* azole resistance – *RPN4* and *MAR1* - and biofilm formation – *EFG1* and *TEC1* -, using an optimized CRISPR-Cas9 system to delete the genes in question and, subsequently, analyse the phenotypic consequences of these mutations in *C. glabrata* cells.

MATERIALS AND METHODS

Strains and culture media

C. glabrata single deletion mutant KCHr606_Δ*ura3* strain was used in all the experiments involved in CRISPR-Cas9-mediated gene deletion. The *C. glabrata* L5U1 strain was also used. Yeast cells were cultured in Yeast-Pentose-Dextrose (YPD) medium (Yeast Extract: 20g/L; Peptone: 10g/L; Glucose: 20g/L), Minimal Medium Broth (MMB) medium (Glucose: 20g/L; Ammonium Sulfate: 2,7g/L; Yeast Nitrogen Base without amino acids and ammonium sulfate: 1,7g/L) or MMB medium supplemented with adenine (3mg/L or 20mg/L), when required. DH5α *E. coli* cells were grown in Luria-Bertani (LB) medium or LB medium supplemented with ampicillin (150mg/L), when required. Liquid cultures were grown with orbital agitation (250rpm) at 30ºC (yeast) or 37º (*E. coli*). Solid media were achieved by adding 20g/L agar to each respective medium.

Plasmids, sgRNA design and cloning

The plasmid used throughout the CRISPR-Cas9 system experiments was the *S. cerevisiae* and *C. glabrata* Solo CRISPR vector pV1382 developed by Vyas *et al*[21]. For site-directed mutagenesis of the *RSB1* promoter, the plasmid used was pYEP354_*CgRSB1*prom_*lacZ*, an expression fusion plasmid in which the *RSB1* promoter region fused with a *lacZ*-coding sequence at the pYEP354 basal vector. A list of *C. glabrata* genes and correspondent guide sequences with no off-targets was obtained from Vyas *et al*[21] (http://osf.io/ARDTX/). With the off-target effects excluded, the gRNAs were chosen based on the on-target score (on-target activity calculated with the Rule Set 2 from Doench J. *et all*[22]), with higher scores being more favourable. Following the criteria of Vyas *et al*[21], the gRNA sequences – forward (Fw) and reverse (Rv) - for three different target genes (*ADE2*, *RPN4*, *EFG1*, *MAR1* and *TEC1*) were designed: *CgADE2* (*CAGL0K10340g*) ACAACACAAGGCCAAATTAA; *CgRPN4* (*CAGL0K01727g*) AGGATGAGCTGTACAATATG; *CgEFG1* (*CAGL0M07634g*) ACACATACTTACCCCCACCA; *CgMAR1* (*CAGL0B03421g*) AGAGCGATGAGTAACCCTGT; *CgTEC1* (*CAGL0M01716g*) AAAGTACCCATGTCTAACAC.

Because the gRNAs will be inserted in the pV1382 between the promoter *SNR52* and the gRNA scaffold sequence, the restriction enzyme chosen for plasmid digestion was BsmBI. To clone the sgRNA into the BsmBI-digested expression vector, two oligonucleotides (forward and reverse) were synthesized with 4 nucleotides in the 5' end and one nucleotide in the 3' end that are compatible with the ends of the BsmBI-digested vector. Considering this, the complete sgRNA sequences, with the plasmid nucleotides (italic) flanking the 20 nucleotide guide sequences (bold), are the following:

Guide_*CgADE2*_TOP – Fw:
5'-*GATCG***ACAACACAAGGCCAAATTAA***G*-3'
Guide_*CgADE2*_BOT – Rv (reverse complemented):
5'-*AAAAC***TTAATTTGGCCTTGTGTTGT***C*-3'
Guide_*CgRPN4*_TOP – Fw:
5'-*GATCG***AGGATGAGCTGTACAATATG***G*-3'
Guide_*CgRPN4*_BOT – Rv (reverse complemented):
5'-*AAAAC***CATATTGTACAGCTCATCCT***C*-3'
Guide_*CgEFG1*_TOP – Fw:
5'-*GATCG***ACACATACTTACCCCCACCA***G*-3'
Guide_*CgEFG1*_BOT – Rv (reverse complemented):
5'-*AAAAC***TGGTGGGGGTAAGTATGTGT***C*-3'

Guide_*CgMAR1*_TOP – Fw:
5'-*GATCG***AGAGCGATGAGTAACCCTGT***G*-3'
Guide_*CgMAR1*_BOT – Rv (reverse complemented):
5'-*AAAAC***ACAGGGTTACTCATCGCTCT***C*-3'
Guide_*CgTEC1*_TOP – Fw:
5'-*GATCG***AAAGTACCCATGTCTAACAC***G*-3'
Guide_*CgTEC1*_BOT – Rv (reverse complemented):
5'-*AAAAC***GTGTTAGACATGGGTACTTT***C*-3'

Although the guiding sequences for CRISPR-mediated deletion of the *MAR1* and *TEC1* genes were designed, further steps (cloning into the plasmid and so on) were not achieved.

The protocol used for cloning the sgRNA into pV1382 included plasmid digestion (2µg plasmid DNA) with the enzyme BsmBI (10U), anneal of sgRNA oligos (100µM each oligo; negative control without oligos), ligation of sgRNA into the plasmid (40ng of plasmid DNA; 1µL of the annealed sgRNA) and DH5α cells transformation by heat shock. Selection was made on LB medium plates with ampicillin. The primer for confirmation of a successful sgRNA cloning on pV1382 consists of a 20 nucleotides sequence present in the *SNR52* promoter a few nucleotides upstream the BsmBI restriction site: 5'-GCTGTAGAAGTGAAAGTTGG-3' (9908-9927 of pV1382).

Repair template design and construction

To create the repair template cassette, two primers were designed with a 20 nucleotide TAG sequence identified in bold (primer *ScADE2* deletion in Vyas *et al*[21]) and 40 nucleotides upstream (primer forward) and downstream (primer reverse) the target gene, identified in italic, known as the homology arms:

RT_*CgADE2*deletion_TOP – Fw: 5'-*TGTTACCAA CGATACAGGTTTATTTTGCTTACGAATAATA***GAGGGG GACATATATAAGTT**-3'

RT_*CgADE2*deletion_BOT – Rv (reverse complemented): 5'-*GAATTTCAAGCAAAGACTAACTGGT TTTATAGATGGTGCT***AACTTATATATGTCCCCCTC**-3'

RT_*CgRPN4*deletion_TOP – Fw: 5'-*CAATTCTAT TAAAACTTTCCTCTCGAGAGCGGTAACGAGG***GAGGG GGACATATATAAGTT**-3'

RT_*CgRPN4*deletion_BOT – Rv (reverse complemented): 5'-*TCCGAAATTTTAAAAGAAATTTGAAT GATGTTGGGGGTAT***AACTTATATATGTCCCCCTC**-3'

RT_*CgEFG1*deletion_TOP – Fw: 5'-*GGTTAATGAGCG TAGACTTGAACTGAAAAGAAAATGTGCG***GAGGGGG ACATATATAAGTT**-3'

RT_*CgEFG1*deletion_BOT – Rv (reverse complemented): 5'-*GTTATACAATGGTACATAGCGATTC ATTACGAATATTAAG***AACTTATATATGTCCCCCTC**-3'

RT_*CgMAR1*deletion_TOP – Fw: 5'-*TTAAGTATTCCGC TATACTCACTGTACCCTAAAGACGACA***GAGGGGGA CATATATAAGTT**-3'

RT_*CgMAR1*deletion_BOT – Rv (reverse complemented): 5'-*CTGTGGAAAAATTAAATACACAAAC ATAACAAATGCACAC***AACTTATATATGTCCCCCTC** -3'

RT_*CgTEC1*deletion_TOP – Fw: 5'-*ATCGTACTCCCCC CCACAAATAACGCCCTCAATCTATATT***GAGGGGGAC ATATATAAGTT**-3'

RT_*CgTEC1*deletion_BOT – Rv (reverse complemented): 5'-*TCTGCAGAAAAAATAAAAATGTAGCATTCCTACATC TCTC***AACTTATATATGTCCCCCTC**-3'

The repair template cassettes designed for *MAR1* and *TEC1* gene deletion were not generated.

Yeast cells transformation and screening for genetic modification

Yeast cells were cultured in YPD medium. Transformation with pV1382_guide*ADE2* and repair template was tested with two different protocols, the Lithium Acetate method (kit MP biomedicals) and the Transformation of Expression Vectors into Yeast protocol from Gietz and Woods. Transformation with pV1382_guide*RPN4* and pV1382_guide*EFG1* with corresponding repair templates was carried out following the Lithium Acetate method (kit MP biomedicals). Cells where then plated in appropriate selection medium (MMB without uracil for *RPN4* and *EFG1* deletion mutants and MMB without adenine and uracil for *ADE2* deletion mutants) and incubated at 30ºC for 5-8 days (as needed) until colony growth. The detection of colonies genetically modified in *C. glabrata ADE2* deletion mutant plates was possible through visual confirmation since these colonies displayed a red pigmentation. For *C. glabrata RPN4* and *EFG1* deletion confirmation, a screening assay was needed. The DNA of candidate colonies was extracted as described below, followed by PCR amplification of the modified target *locus*. The primer forward used to confirm a successful gene deletion corresponds to the TAG sequence, which is expected to be inserted in the *locus* of the gene targeted for deletion: 5'-GAGGGGGACATATATAAG TT-3'. The primer reverse corresponds to a selected region downstream of the gene targeted for deletion, in this case *CgRPN4* and *CgEFG1*:

***CgRPN4*_deletion_conf_Rv**:
5'-CTGAGCTTGCTAAGATCAAT-3'
***CgEFG1*_deletion_conf_Rv**:
5'-CATGCCAAATCCCTATACTA-3'

DNA extraction

All experiments considering plasmid extractions from *E. coli* were carried out using the NZYMiniprep kit. For DNA extraction from *C. glabrata*, a different procedure was followed: biomass from the grown colonies was collected and added to 200 µL of lysing buffer with 0.5 mm glass beads, followed by vortex and then incubated for 1h

at 65ºC. After resting in ice for 2 minutes, a 15-minute 13 000 rpm centrifugation at 4ºC followed, and the supernatant was transferred to a tube containing 1/10 of the supernatant volume of Sodium Acetate (3M, pH 4.8) and 2 volumes of absolute ethanol. This mixture was stored at -20ºC for 30 minutes and then centrifuged for 20 minutes, 13000rpm at 4ºC. The DNA pellet was washed with 500µL 70% ethanol, followed by an 8-minute 13000rpm centrifugation at 4ºC and ethanol evaporation through speed vacuum. The DNA was resuspended in water.

Cloning of the *CgRBS1* promoter and site-directed mutagenesis

The pYPE354 plasmid was used as described before to clone and express the *lacZ* reporter gene. pYEP354 contains the yeast selectable marker *URA3* and the bacterial selectable marker *AmpR* genes. *CgRSB1* promoter DNA was generated by PCR, using genomic DNA extracted from the sequenced CBS138 *C. glabrata* strain, and primers forward 5'-CCGGAATTCCGTACACAAGCAGC TAGGTAAT-3' and reverse 5'-AACTGCAGCTCATCCATCAT TAGTTATT-3'. The first primer contains a region with homology within the beginning of the *CgRSB1* promoter and a recognition site for the EcoRI restriction enzyme, flanked by additional bases. The second primer contains a region with homology within the end of the *CgRSB1* promoter and the beginning of the *CgRSB1* coding sequence and a recognition site for the PstI restriction enzyme, flanked by additional bases. The amplified fragment was ligated into the pYEP354 vector (T4 Ligase, New England Biolabs), previously cut with the same restriction enzymes, to obtain the pYEP354_*CgRSB1*prom_*lacZ* plasmid. The putative CgRsb1 consensus in the *CgRSB1* promoter was mutated by site-directed mutagenesis using the following primers for each motif: motif 1 (fw) 5'-GACCCGAGGTGT TTCCAAAATCGGTCCCACGCTC-3', (rv) 5'-GAAGCG TGGGACCGATTTTGGAAACACCTCGGGTC-3'; motif 2 (fw) 5'-CTCAGAAATTGGGGTTGGGGGGGAGGGA TG-3', (rv) 5'-CATCCCTCCCCCCCAACCCCAATTTCT GAG-3'; motif 3 (fw) 5'-GAAATTGGGGGAGGGGGGTT GGGATGAGGTGGAAGTG-3', (rv) 5'-CACTTCCACCT CATCCCAACCCCCCTCCCCCAATTTC-3'; motif 4 (fw) 5'-CATCGCAAGGAATAATAACCGGGATGTAGT ACAATAGTGGTTC-3', (rv) 5'-GAACCACTATTGTAC TACATCCCGGTTATTATTCCTTGCGATG-3'. The designed primers contain two mutations within each four of the potential consensus, resulting in the production of each the mutated consensus by PCR amplification to obtain the pYEP354_mut_*CgRSB1*prom_*lacZ* plasmids. The original template was then degraded by DpnI digestion.

For the PCR for site-directed mutagenesis of the *RSB1* promoter, 1µL of each primer (forward and reverse) were added to 2µL of the plasmid DNA (30ng/µL), 10µL of HF buffer (5x), 2µL of Mg^{2+}, 0,5µL of Phusion polymerase, 1µL of dNTPs, 1,5µL of DMSO and H_2O up to a total amount of 50µL per reaction. The temperature of annealing depends on the primers used:

Primers for motif 1: $T_{annealing}$ = 63ºC

Primers for motifs 2 and 3: $T_{annealing}$ = 62ºC

Primers for motif 4: $T_{annealing}$ = 58ºC

RT-PCR gene expression measurement

The transcript levels of the *CgRSB1* or the *lacZ* reporter gene encoding for β-galactosidase were determined by quantitative real-time PCR (RT-PCR). L5U1 cells transformed with the pYEP354_*CgRSB1*prom_*lacZ* or each pYEP354_mut_*CgRSB1*prom_*lacZ* plasmids were grown in BM supplemented with leucine until mid-exponential phase. Fluconazole exposure, cell harvesting and storage were performed as mentioned above. For total RNA extraction, the hot phenol method was applied[23]. Synthesis of cDNA for real time RT-PCR experiments, from total RNA samples, was performed using the Multiscribe™ reverse transcriptase kit (Applied Biosystems) and the 7500 RT-PCR Thermal Cycler Block (Applied Biosystems), following the manufacturer's instructions. The quantity of cDNA for the following reactions was kept around 10 ng. The subsequent RT-PCR step was carried out using SYBR® Green (NZYTech) reagents with default parameters established by the manufacturer and the primers forward 5'-TGGCTGGAGTGCGATCTTC-3' and reverse 5'-CGTGCATCTGCCAGTTTGAC-3'. The *CgRDN25* gene transcript levels were used as an internal reference (primers forward 5'-AACAACTCACCGGCCGAAT-3' and reverse 5'-CAAGCGTGTTACCTATACTCCGCCGTCA-3').

RESULTS

CRISPR-Cas9 system implementation and optimization in *C. glabrata*

The functional characterization of a gene to understand the mechanisms underlying its mode of action becomes possible with the use of advanced genetic manipulation tools, where the CRISPR-Cas9-based editing system has emerged as a particularly powerful tool successfully applied in a variety of organisms, from microorganisms to human cells.

The CRISPR-Cas9 system operates with the endonuclease protein Cas9 for RNA-guided DNA recognition and cleavage, representing a system with high specificity very used for genome engineering applications[24]. By modifying a 20-nucleotide sequence at the 5' end of sgRNA, it is, in principle, possible to target any desired gene. However, when selecting the target sequence of a gene, there are a few things that need to be considered. The first consists in the presence of a PAM sequence immediately downstream of the target sequence, which could be a limitation when editing the genome of AT-rich organisms. Another concern is minimising off-target effects that trigger unintended mutations within the genome, and to do so, the target sequence must be unique throughout the genome. Also, to achieve effective gene knock-out, it is recommended that the target sequence be within the first

half of the gene since the targeting of 3' exons could fail to obtain complete inhibition of gene function[25]. Nonetheless, appropriate target recognition by sgRNA in the CRISPR-Cas9 system is rather specific, with decreases in Cas9 cleavage activity when a single nucleotide mismatch occurs in the sgRNA sequence[25].

The initial goal of this work consisted in the implementation and optimization of a CRISPR-Cas9 system for gene deletion via homology-directed repair (HDR) in *C. glabrata*, and it was based on the work of Vyas *et al*[21]. Here, a single-plasmid CRISPR system was used, providing also a repair template cassette to increase the efficiency of homologous recombination in *C. glabrata*, since the dominant DNA repair pathway of this yeast is NHEJ[21]. The main advantage of this system over the previous ones developed for *C. glabrata* is the use of a solo vector (pV1382) expressing both *CAS9* and sgRNA. The several selection markers found in this solo vector are also advantageous to use in a wider range of strains: a *URA3* marker that can be used for counterselection in *ura3* auxotrophs, the dominant-selectable *NAT1* gene, which confers resistance to the drug nourseothricin (NAT^R) and the ampicillin resistance gene (*ampR*) that is used for selection of transformed *E. coli*[21].

The first step of a CRISPR project begins with the design of sgRNA, a short synthetic RNA composed of a scaffold sequence responsible for Cas9 binding, and a targeting sequence consisting of a ~20 nucleotides spacer that guides the Cas9 and binds to the target DNA *locus*[26]. For Cas9 to cleave the DNA, it is essential that the target *locus* is located immediately after the 5' of a short protospacer adjacent motif (PAM) sequence containing a 5'-NGG-3' (the canonical PAM sequence, where "N" is any nucleotide) in the non-target strand, but not in its target-strand complement[27,28]. However, this PAM sequence should not be included as a part of the sgRNA. The sgRNA sequences used were chosen from the guide compilation tables designed by Vyas *et al*[21] that included the guide sequences corresponding to each annotated gene in the genome of *C. glabrata*, with exception of target sequences that had 6 instances of T in the 20 nucleotides before the NGG as it would lead to premature termination from polymerase (Pol) III promoters (such as *SNR52*)[29].

Optimization of sgRNA cloning (*CgADE2*) into pV1382 in *E. coli* DH5α cells

The *ADE2* gene was chosen as a proof-of-concept platform to optimize a CRISPR-Cas9 system for gene deletions in *C. glabrata*, since the disruption of *ADE2* in this yeast results in the accumulation of a red-pigmented intermediate due to blocking of adenine biosynthesis, allowing visual identification of the *C. glabrata* Δ*ADE2* colonies[30].

The protocol of cloning a sgRNA into pV1382 started with the plasmid digestion with the restriction enzyme BsmBI (Figure 1). Here, three different conditions were tested as it is represented in Table 1. The oligos used to produce the sgRNA sequence were annealed and ligated into the linearized pV1382 plasmid, giving rise to pV1382_guideADE2. During the ligation of sgRNA into the vector, a negative control was prepared where no sgRNA oligos were added to the vector ligation mixture. When the plasmid is digested and opened, it is no longer active. Since the restriction enzyme used for digestion (BsmBI) does not create complementary sticky ends in the plasmid, it cannot re-circularize on its own. For the re-circularization to occur, it would either be due to the presence of the initial fragment or with a guide sequence added, but in the negative control there is no addition of sgRNA oligos. Therefore, in these plates the chance of plasmid re-circularization and, therefore, re-activation is lower, meaning the number of colonies grown is expected to be lower than in the sample plates.

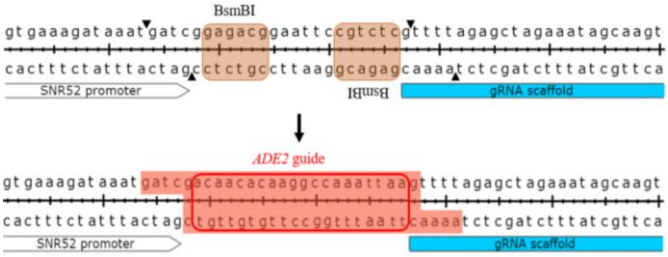

Figure 1 - Cloning of *ADE2* guide sequence into pV1382: plasmid digestion with BsmBI (sequences of recognition shaded in brown) is followed by ligation of annealed oligos (red shaded sequences) with desired guide sequence

Following transformation of *E. coli* cells with pV1382_guide*ADE2*, selection of transformants was achieved by plating the cells in LB medium with ampicillin. The number of colonies grown in each plate is shown in Table 1:

Table 1 - Different plasmid digestion conditions with corresponding number of colonies grown in each plate.

		Plasmid digestion with BsmBI		**Transformation of DH5α (nº CFUs)**	
pV1382 _guide*ADE2*		Incubation temperature (ºC)	Incubation time (min)	Sample	Negative control
	1.	55º	10	18	19
	2.	55º	60	26	7
	3.	37º	30	35	70

Comparing the number of colonies between the samples and the respective negative controls, it is seen that the results of both digestion conditions number 1 (55ºC, 10min) and 3 (37ºC, 30min) are invalid, since it was expected that the number of colonies in the sample plates would be significantly higher than the number of colonies in the negative control. This is the case of the plates in condition 2., so this protocol was selected for further work, as is proved to be the most suitable for the BsmBI restriction activity. The NZYMiniprep kit was used for plasmid

extraction from candidate colonies (sample plate 2.) and the successful sgRNA cloning was confirmed by sequencing. Sequencing results revealed the cloning of the sgRNA into pV1382 was successful, which permitted the use of pV1382_guide*ADE2* in CRISPR-Cas9 mediated gene deletions.

Using a CRISPR-Cas9 system for *CgADE2* disruption

For CRISPR-Cas9 mediated *ADE2* gene deletion in a URA$^-$ strain (KCHr606_Δ*ura3*), two different yeast transformation protocols were tried out. In the first three assays, the Alkali-Cation Yeast Transformation kit protocol from MP Biomedicals was used. In the fourth assay, the Transformation of Expression Vectors into Yeast protocol (Gietz and Woods, 2000) was followed. Distinct cell concentrations were tested in the transformation reactions, with best results being achieved with cultures grown to OD 0.6-0.8. To determine the range of DNA that leads to higher transformation efficiency, the transformation assays were performed with different amounts of DNA, as it is represented in Table 2. Two different concentrations of adenine in MMB medium were also tested, and the results show that cells grew only when transformed with amounts of pV1382_guide*ADE2* above 1µg and plated in a medium with 20mg/L of adenine instead of 3mg/L. The presence of adenine is required so that the successfully edited strains (ADE-) are able to grow in the transformation plate. The absence of uracil in the MMB medium allows for the selection of transformed cells, since the strain of *C. glabrata* used is Δ*ura3*. Different amounts of repair template aimed at *CgADE2* deletion for the generation of knockout strains were also tested. It seems that 3µg is enough to achieve its purpose. The presence of red/pink colonies (Figure 2), which corresponds to the Δ*ade2* phenotype, revealed the CRISPR-Cas9 *ADE2* deletion was successful in numerous colonies. Both transformation protocols displayed a successful outcome, although the number of colonies obtained using the MP Biomedicals transformation kit was significantly higher (Table 2). To confirm the Δ*ade2* phenotype, several colonies were collected and plated in MMB medium, this time without adenine. The absence of colonies grown in this plate supported the idea that *ADE2* was successfully deleted.

Table 2 - Results of different transformation protocols of *C. glabrata* cells using a CRISPR-Cas9 system for *ADE2* deletion

	pV1382_ guideADE2 (µg)	Repair template (µg)	Transformation Plates Medium	Colonies	Red colonies	Total nº colonies	% genetically engineered colonies	Transformation Protocol
1st assay	0,3	5	MMB + Adenine (3mg/L)	No	-	-	-	Alkali-Cation Yeast Transformation kit (MP Biomedicals)
	0,5	5	MMB + Adenine (3mg/L)	No	-	-	-	
2nd assay	0,5	5	MMB + Adenine (3mg/L)	No	-	-	-	
	0,7	5	MMB + Adenine (3mg/L)	No	-	-	-	
3rd assay	1	3	MMB + Adenine (3mg/L)	No	-	-	-	
	2	3	MMB + Adenine (3mg/L)	No	-	-	-	
	3	3	MMB + Adenine (3mg/L)	No	-	-	-	
	1	3	MMB + Adenine (20mg/L)	Yes	42	217	19,35%	
	2	3	MMB + Adenine (20mg/L)	Yes	54	314	17,20%	
	3	3	MMB + Adenine (20mg/L)	Yes	27	179	15,10%	
4th assay	1	3	MMB + Adenine (20mg/L)	Yes	3	16	18,7%	Transformation of Expression Vectors into Yeast (Gietz and Woods, 2000)
	2	3	MMB + Adenine (20mg/L)	Yes	10	40	25%	
	3	3	MMB + Adenine (20mg/L)	Yes	9	24	37,5%	

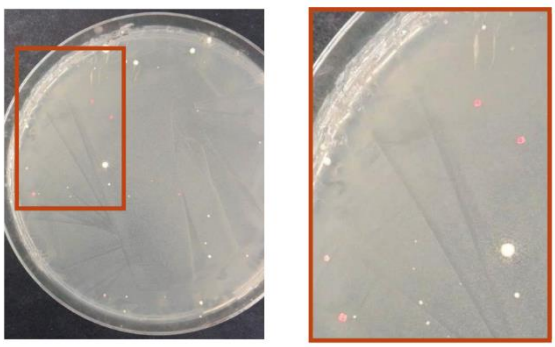

Figure 2 - C. glabrata KCHr606_Δura3 strain transformed with pV1382_guideADE2 and repair template for CRISPR-Cas9 mediated ADE2 gene deletion. The brown box presents a magnified view of red/pink colonies from the left figure

Application of a CRISPR-Cas9 system to C. glabrata gene characterization

A CRISPR-Cas9 system, previously optimized and implemented in *C. glabrata* for *ADE2* gene deletion, was used in the attempt to generate several deletion mutants in a *C. glabrata* URA$^-$ strain (KCHr606_Δ*ura3*) in order to further investigate and functionally characterize the deleted genes.

For this work, *EFG1* and *TEC1* were selected, aiming the analysis of their role in biofilm formation, whereas *RPN4* and *MAR1* were chosen for being potentially involved in azole antifungal resistance in *C. glabrata*.

gRNAs and repair templates were designed for the deletion of the above mentioned four genes, however, the CRISPR-Cas9 system and further steps could only be applied to *EFG1* and *RPN4*, as a consequence of the COVID-19 pandemics that forced the laboratory work to end sooner than expected.

CRISPR-Cas9 mediated *EFG1* gene deletion

The cloning of the corresponding sgRNA into pV1382 was performed as previously described for the deletion of *CgADE2*, as was the construction of the repair template designed for gene deletion.

Transformation of *C. glabrata* cells (using the Alkali-Cation Yeast Transformation kit protocol) with the plasmid and the repair template was carried out and colonies were obtained. The DNA from the colonies corresponding to potential CRISPR-Cas9-generated *C. glabrata* Δ*efg1* deletion mutant strains was extracted and sequenced, revealing that the intended genome editing was achieved.

With the generated Δ*efg1* mutant strain, it is now possible to carry out biofilm quantification assays to test whether *C. glabrata*'s ability to form biofilm is affected in the absence of *EFG1*. Unfortunately, this step could not be accomplished as a result of a sudden loss of access to the laboratory to continue investigations, caused by the COVID-19 pandemics. A biofilm quantification assay would allow for a possible confirmation of an involvement of *EFG1* in the mechanisms underlying biofilm formation, as it is expected a biofilm reduction in the Δ*efg1* mutant strain compared to wild-type. Furthermore, to verify if the outcome of this assay is directly related to the *EFG1* gene or if it represents an indirect result, a phenotypic complementation would be carried out by introducing an *EFG1* expression plasmid in the *C. glabrata* Δ*efg1* mutant strain and comparing biofilm phenotypic results between the complemented and mutant strains.

CRISPR-Cas9 mediated *RPN4* gene deletion

Following the protocols formerly applied, a CRISPR-Cas9 system was implemented in *C. glabrata* to generate Δ*rpn4* strains, providing a repair template to be inserted at the DNA break site.

Confirmation of the intended gene deletion was achieved by PCR, carried out over DNA extracted from potential *C. glabrata* Δ*rpn4* colonies, followed by an electrophoresis that shows several colonies with a PCR product consistent with what would be expected for a positive gene deletion. However, confirmation by DNA sequencing was not yet obtained as a result of a sudden loss of access to the laboratory to continue investigations, caused by the COVID-19 pandemics.

Once the Δ*rpn4* mutant strain is confirmed, the next step would be to engage in antifungal susceptibility assays. As it was mentioned above, this step of the experimental work could not be done, although it would be of great interest to carry on investigations about the role of *CgRPN4* in antifungal resistance. Though it has been shown that the deletion of *RPN4* generated *C. glabrata* mutants with increased susceptibility to azoles[31], what was planned was the generation of multiple deletion mutants of genes presumed to be involved in antifungal resistance - Δ*rpn4* Δ*mar1* Δ*pdr1*. This approach of combining mutations would help perceiving the interactions between these specific genes when compared to individual mutations.

Site-directed mutagenesis of possible Mar1 binding sites in the *RSB1* promoter

To assess whether the predicted *RSB1* promoter response elements for the TF Mar1 where indeed correct, specific mutations were introduced in each one of these four potential recognition motifs through site-directed mutagenesis. Following this procedure, activation of the *RSB1* promoter - cloned in the plasmid pYEP354 immediately before the reporter gene *lacZ* - was measured by quantifying the expression of *lacZ* with RT-PCR. Furthermore, the *RSB1* promoter activation was measured in the presence and absence (control) of fluconazole, as Mar1 is suspected to play a role in gene regulation in response to azole-induced stress. The results obtained are represented in Figure 3.

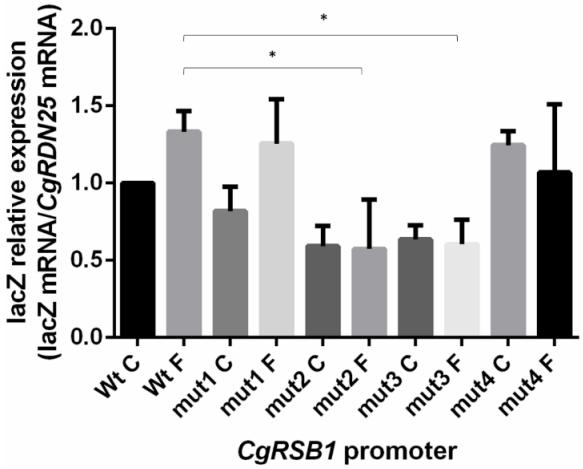

Figure 3 – Comparison of CgRSB1 promoter activation, in the presence (F) and absence (C) of fluconazole, between cells containing the wilt-type (Wt) promoter and the promoter mutated in motifs 1-4 (mut1-mut4). Activation was measured through the relative expression of the reporter gene lacZ.

To understand if the *RSB1* promoter motifs affect the basal expression of the gene, it is necessary to compare the expression of *lacZ* between the *wild-type* promoter and the mutated motifs in control conditions. Statistical analysis did not show a significant difference in the activation levels of the control mutated promoters compared to the control *wild-type*, hence, it is possible to assume that the four selected *RSB1* promoter motifs do not affect the basal expression of *RSB1*. On the other hand, in the presence of fluconazole it is possible to detect considerable variations in the promoter activation. When analysing the data from Figure 3, it is seen that mutations in motifs 2 and 3 (mut2 and mut3) of the *RSB1* promoter reduce its activation in the presence of fluconazole when comparing with the *wild-type* promoter (highlighted in Figure 3 with *). These results

suggest that motifs 2 and 3, both sharing the same sequence – GGGGAGG -, of the *RSB1* promoter are potentially involved in the expression of *RBS1* when fluconazole is present in the medium.

A further evaluation of this regulation mechanism can be achieved with the use of Chromatin Immunoprecipitation (ChIP), a method that will confirm whether the TF Mar1 actually binds to these two motifs of the *RSB1* promoter in order to activate *RSB1*.

DISCUSSION AND FUTURE PERSPECTIVES

This study describes how an innovative genome editing technology like the CRISPR-Cas9 system can be used as a valuable tool for the functional characterization of numerous *C. glabrata* genes presumed to be involved in this pathogen's virulence and antifungal drug resistance mechanisms.

The CRISPR-Cas system is considered to be one of the major breakthrough discoveries of genetics, currently being explored for genome edition of a great deal of organisms. A CRISPR-Cas based approach has several advantages compared to the already existing genome engineering techniques. For instance, while being robust, this technology is very user-friendly since it only requires the construction of a recombinant plasmid containing the sequences coding for the Cas9 protein and the gRNA, a target-specific small guide sequence. As a consequence, this approach is less time-consuming, which is a very valuable asset. The design of the gRNA allows for the targeting of a vast number of genes, provided they are located next to a PAM sequence. This requirement is, however, a restriction for the targetable genomic loci. There are already quite a few studies developing approaches to expand the targeting range of CRISPR-Cas9, for example through protein engineering of Cas9 to alter PAM recognition[32].

The first part of this work consisted of the implementation and optimization of a CRISPR-Cas9 system, previously developed by Vyas *et al*[21], to implement in the *C. glabrata* KCHr606_Δ*ura3* strain for gene deletions. This system was chosen mainly because of the advantages of using a solo vector that encodes both Cas9 and the gRNA, this way facilitating cell transformation. One important aspect to minimize the off-target effects by the CRISPR-Cas9 system is the off-target prediction. Here, adequate gRNA design was carried out according to a list of *C. glabrata* genes and guiding sequences, provided by Vyas and colleagues, with the predicted off-target sites.

A series of optimization steps were carried out, starting with the testing of different incubation conditions for plasmid digestion to achieve a suitable outcome of gRNA cloning into the plasmid. Once the solo vector containing the designed gRNA and Cas9 coding sequences was obtained, the optimization of the CRISPR-Cas9 system itself began. During the transformation of *C. glabrata* cells with the solo vector, a repair template was also supplied in order to increase the odds of the HDR pathway to act upon the CRISPR-Cas9-generated DSB. Two different transformation protocols were tried out and optimized for CRISPR-Cas9 mediated *ADE2* gene deletion in *C. glabrata* until the desired outcome, which in this case was obtaining red colonies (Δ*ade2* phenotype), was achieved. It has been demonstrated that the NHEJ pathway is the dominant repair pathway following a DSB in *C. glabrata*[21], however, supplying a repair template was shown to, at a certain level, circumvent this tendency and favour the action of the HDR pathway. Even though the percentages of efficiency obtained for gene deletion using this CRISPR-Cas9 system were not as high as expected, the results were satisfactory enough to carry on with CRISPR-mediated deletions of a number of *C. glabrata* genes of interest to be further studied. The higher percentage of genome editing efficiency obtained in the study of Vyas and colleagues[21], from which the CRISPR-Cas9 system used in this work was based on, could be partially related to the yeast transformation protocol they followed, consisting of a combination of a lithium acetate and electroporation protocol. Here, the transformation of *C. glabrata* did not include the electroporation step, but the use of lithium acetate followed by heat-shock treatment (among other steps described in the protocols referred in the 'Materials and Methods' section).

With countless studies recognising *C. glabrata* as an emerging human pathogen[4–6], understanding its virulence mechanisms became an important concern for public health. *C. glabrata* was shown to have an intrinsically low susceptibility to azole antifungal drugs[3,5,33–35], also being the main *Candida* species exhibiting multidrug resistance[9]. The fast azole resistance acquisition seen in *C. glabrata* has been associated with gain-of-function mutations in *PDR1*[12,36,37], and results such as the upregulation of *CgRPN4* seen in fluconazole-resistant Pdr1 gain-of-function mutants of *C. glabrata*[38], among other, led to the idea of a possible link between *CgRPN4* and azole resistance in this pathogen. Therefore, *CgRPN4* was chosen to be further studied in this work, that began with its deletion using the previously optimized CRISPR-Cas9 system. From the colonies obtained, several were considered potential *C. glabrata* Δ*rpn4* mutants according to the confirmation PCR and electrophoresis. It was not possible, however, to confirm a successful CRISPR-Cas9-mediated *RPN4* deletion through DNA sequencing due to unexpected loss of laboratory access as a consequence of the COVID-19 pandemics. Assuming the intended gene deletion was achieved, the next phase planned for this part of the work would be to create, again using the CRISPR-Cas9 system, a *C. glabrata* Δ*rpn4* Δ*mar1* Δ*pdr1* multiple deletion mutant and, later on, carry out azole susceptibility assays, as all three genes are presumed or known to play a role in antifungal resistance.

Another known virulence feature of *C. glabrata* is its ability to form biofilms, in which the *EFG1* and *TEC1* genes are presumed to play a role[39]. For further

characterization, both genes were planned to be deleted in *C. glabrata* using the CRISPR-Cas9 system, yet only the Δ*efg1* deletion mutant was obtained, as the COVID-19 pandemics prevented the *TEC1* gene studies to go beyond the design of its repair template and gRNA. The next phase planned for this part of the work would be to create, again using the CRISPR-Cas9 system, a *C. glabrata* Δ*efg1* Δ*tec1* double deletion mutant and, later on, carry out biofilm formation assay, as both genes are presumed to play a role in this process.

The multiple deletion mutant method would help elucidate the genetic interactions between the deleted genes, more specifically the extent to which the function of one gene depends on the presence of a second or third genes. The existence of such genetic interactions can be inferred when the loss of the group of genes has a stronger phenotypic effect than the loss of any of the genes alone[40], thus facilitating the identification and characterization of gene functions and cellular pathways[41]. Additionally, since the single and multiple deletion strains were being built in a *URA3*- background, it would further be possible to confirm gene functions through gene expression complementation.

The recently discovered potential link between the uncharacterized CgMar1 TF and fluconazole stress responses, uncovered through previous unpublished work from our team, encouraged a deeper analysis of this protein's functions, which led to the hypothesis of Mar1 being a transcriptional regulator of *RSB1*, binding to its promoter in response to fluconazole-induced stress. The results from the RT-PCR analysis of the *RSB1* promoter activation, where a comparison is made between the *wild-type* promoter and four mutated possible Mar1-binding motifs, showed that in control conditions these motifs are not relevant for the basal expression of *RSB1*. However, two of the motifs, specifically motifs 2 and 3 (both with the GGGGAGG sequence) were shown to influence *RSB1* gene expression when fluconazole was added to the medium. This outcome supports the theory of Mar1 being involved in fluconazole stress responses mediated, at least partially, by *RSB1*. However, confirmation of whether or not Mar1 binds to the two *RSB1* promoter motifs recognized as relevant for this matter is still needed. This confirmation would be achieved with ChIP, a method that includes the crosslink between the Mar1 protein and its DNA binding sites, followed by chromatin shearing into short fragments and isolation of the DNA-interacting protein (crosslinked to DNA) by immunoprecipitation[42]. The protein binding sites, after protein release are amplified with PCR and sequenced. Again, due to the COVID-19 pandemics, this step could not be accomplished. Even though the closest Mar1 ortholog found is the *S. cerevisiae* Hap1 TF, the GGGGAGG motif is not included in the list of known Hap1 consensus binding sites[43], supporting the idea of these proteins having different functions. Interestingly, the GGGGAGG sequence is found in the promoter regions of *CgSNQ2*, a drug efflux pump from the ABC superfamily, and *CgQDR2*, a MFS transporter, both known to be involved in azole resistance mechanisms in *C. glabrata*. This finding could, perhaps, point towards the involvement of Mar1 in *SNQ2* and *QDR2* regulation, in the presence of fluconazole, through the binding to the mentioned motif, although previous RNA-seq analysis done in our lab (Pais *et al*, unpublished results) did not seem to support this idea. Additionally, the GGGGAGG motif is also present in the *C. albicans RTA2* promoter region, a *CgRSB1* ortholog that encodes a protein known to mediate azole resistance responses[44]. Having seen how the GGGGAGG motif affects *CgRSB1* gene expression in the presence of fluconazole, it is possible that this motif has a similar effect in the expression of *RTA2* in *C. albicans* under such conditions, and if so, it would be interesting to find the TF - possibly a Mar1 ortholog - responsible for the regulation of *RTA2* by binding to the said motif. All of these theories require further *in silico* investigations as well as RNA-seq and ChIP assays to confirm possible influences in gene expression and possible TF binding sites.

Altogether, this study provided optimized valuable tools to be applied in the genetic manipulation of *C. glabrata*. Additionally, two putative Mar1 binding sites in the *RSB1* promoter region were uncovered, while two new deletion mutants were obtained, that will contribute to leverage ongoing studies on the mechanisms of biofilm formation and azole resistance in this pathogen.

ACKNOWLEDGEMENTS

This document was written and made publicly available as an institutional academic requirement and as a part of the evaluation of the MSc thesis in Biotechnology of the author at Instituto Superior Técnico. The work described herein was performed at the Institute for Bioengineering and Biosciences of Instituto superior Técnico (Lisbon, Portugal), during the period October 2019-March 2020, under the supervision of Prof. Dr. Miguel Teixeira and co-supervision of Dr. Pedro Pais. I acknowledge Professor Isabel Sá-Correia for the opportunity of joining the Biological Sciences Research Group. This work was supported by the Fundação para a Ciência e a Tecnologia (FCT) (contract PTDC/BIIBIO/28216/2017) as well as by the Programa Operacional Regional de Lisboa 2020 (LISBOA-01-0145 FEDER-022231, the BioData.pt Research Infrastructure). I acknowledge funding received by the iBB from the FCT (UIDB/04565/2020) and from the Programa Operacional Regional de Lisboa 2020 (LISBOA-01-0145-FEDER-007317).

REFERENCES

1. Brown, G. D. *et al.* Hidden killers: Human fungal infections. *Sci. Transl. Med.* **4**, (2012).
2. Pfaller, M. A. & Diekema, D. J. Epidemiology of invasive candidiasis: A persistent public health problem. *Clin. Microbiol. Rev.* **20**, 133–163 (2007).
3. Yapar, N. Epidemiology and risk factors for invasive candidiasis. *Ther. Clin. Risk Manag.* **10**, 95–105 (2014).

4. Antinori, S., Milazzo, L., Sollima, S., Galli, M. & Corbellino, M. Candidemia and invasive candidiasis in adults: A narrative review. *Eur. J. Intern. Med.* **34**, 21–28 (2016).
5. Diekema, D., Arbefeville, S., Boyken, L., Kroeger, J. & Pfaller, M. The changing epidemiology of healthcare-associated candidemia over three decades. *Diagn. Microbiol. Infect. Dis.* **73**, 45–48 (2012).
6. Carreté, L. *et al.* Genome comparisons of Candida glabrata serial clinical isolates reveal patterns of genetic variation in infecting clonal populations. *Front. Microbiol.* **10**, 1–13 (2019).
7. Krcmery, V. & Barnes, A. J. Non-albicans Candida spp. causing fungaemia: Pathogenicity and antifungal resistance. *J. Hosp. Infect.* **50**, 243–260 (2002).
8. Pfaller, M. A., Diekema, D. J., Fungal, I. & Participant, S. Twelve years of fluconazole in clinical practice : global trends in species distribution and fluconazole susceptibility of bloodstream isolates of Candida. *Clin. Microbiol. Infect. Dis.* **10**, 11–23 (2004).
9. Deorukhkar, S. Virulence Markers and Antifungal Susceptibility Profile of Candida glabrata: An Emerging Pathogen. *Br. Microbiol. Res. J.* **4**, 39–49 (2014).
10. Gupta, A., Gupta, A. & Varma, A. Candida glabrata candidemia: An emerging threat in critically ill patients. *Indian J. Crit. Care Med.* **19**, 151–154 (2015).
11. Sandhu, R., Dahiya, S., Sayal, P. & Budhani, D. Increased role of nonalbicans Candida, potential risk factors, and attributable mortality in hospitalized patients. *J. Heal. Res. Rev.* **4**, 78 (2017).
12. Ksiezopolska, E. & Gabaldón, T. Evolutionary emergence of drug resistance in candida opportunistic pathogens. *Genes (Basel).* **9**, (2018).
13. Odds, F. C., Brown, A. J. P. & Gow, N. A. R. Antifungal agents: Mechanisms of action. *Trends Microbiol.* **11**, 272–279 (2003).
14. Deorukhkar, S. C., Roushani, S. & Bhalerao, D. Candidemia due to Non-Albicans Candida Species : Risk Factors , Species Distribution and Antifungal Susceptibility Profile Journal of Microbial Pathogenesis. *J. Microb. Pathog.* **1**, 1–6 (2017).
15. Farmakiotis, D., Tarrand, J. J. & Kontoyiannis, D. P. Drug-Resistant Candida glabrata Infection in Cancer Patients. *Emerg. Infect. Dis.* **20**, 1833–1840 (2014).
16. Uppuluri, P. *et al.* Dispersion as an important step in the Candida albicans biofilm developmental cycle. *PLoS Pathog.* **6**, (2010).
17. Treviño-Rangel, R. de J., Peña-López, C. D., Hernández-Rodríguez, P. A., Beltrán-Santiago, D. & González, G. M. Association between Candida biofilm-forming bloodstream isolates and the clinical evolution in patients with candidemia: An observational nine-year single center study in Mexico. *Rev. Iberoam. Micol.* **35**, 11–16 (2018).
18. Tumbarello, M. *et al.* Risk factors and outcomes of candidemia caused by biofilm-forming isolates in a tertiary care hospital. *PLoS One* **7**, 1–9 (2012).
19. Lane, S., Birse, C., Zhou, S., Matson, R. & Liu, H. DNA Array Studies Demonstrate Convergent Regulation of Virulence Factors by Cph1 , Cph2 , and Efg1 in Candida albicans *. **276**, 48988–48996 (2001).
20. Pais, P. *et al.* Candida glabrata Transcription Factor Rpn4 Mediates Fluconazole Resistance Through Regulation of Ergosterol Biosynthesis and Plasma Membrane Permeability. *Antimicrob. Agents Chemother.* (2020). doi:10.1128/AAC.00554-20
21. Vyas, V. K. *et al.* New CRISPR Mutagenesis Strategies Reveal Variation in Repair Mechanisms among Fungi. *mSphere* **3**, 1–14 (2018).
22. Doench, J. G. *et al.* Optimized sgRNA design to maximize activity and minimize offtarget effects of CRISPR-Cas9. *HHS* **34**, 184–191 (2016).
23. Köhrer, K. & Domdey, H. Preparation of high molecular weight RNA. *Methods Enzymol.* **194**, 398–405 (1991).
24. Doudna, J. A. & Charpentier, E. The new frontier of genome engineering with CRISPR-Cas9. *Science (80-.).* **346**, (2014).
25. Muramoto, T., Iriki, H., Watanabe, J. & Kawata, T. Recent Advances in CRISPR/Cas9-Mediated Genome Editing in Dictyostelium. *Cells* **8**, 46 (2019).
26. Addgene. CRISPR 101: A Desktop Resource. in *Addgene* 307–313 (2017).
27. Sander, J. D. & Joung, J. K. CRISPR-Cas systems for editing, regulating and targeting genomes. *Nat. Biotechnol.* **32**, 347–350 (2014).
28. Anders, C., Niewoehner, O., Duerst, A. & Jinek, M. Structural basis of PAM-dependent target DNA recognition by the Cas9 endonuclease. *Nature* **513**, 569–573 (2014).
29. Vyas, V. K. *et al.* OSF | New CRISPR mutagenesis strategies reveal variation in repair mechanisms among fungi. Available at: https://osf.io/ARDTX/. (Accessed: 19th January 2020)
30. Edlind, T. D. *et al.* Promoter-dependent disruption of genes: Simple, rapid, and specific PCR-based method with application to three different yeast. *Curr. Genet.* **48**, 117–125 (2005).
31. Galocha, M. New players controlling multidrug resistance and biofilm formation in C. glabrata: the important role of Rpn4. (Instituto Superior Técnico - Universidade de Lisboa, 2017).
32. Nishimasu, H. *et al.* Engineered CRISPR-Cas9 nuclease with expanded targeting space. *Science (80-.).* **361**, 1259–1262 (2018).
33. Méan, M., Marchetti, O. & Calandra, T. Bench-to-bedside review: Candida infections in the intensive care unit. *Crit. Care* **12**, 1–9 (2008).
34. Kullberg, B. J. & Arendrup, M. C. Invasive candidiasis. *N. Engl. J. Med.* **373**, 1445–1456 (2015).
35. Bassetti, M., Righi, E., Montravers, P. & Cornely, O. A. What has changed in the treatment of invasive candidiasis? A look at the past 10 years and ahead. *J. Antimicrob. Chemother.* **73**, i14–i25 (2018).
36. Caudle, K. E. *et al.* Genomewide expression profile analysis of the Candida glabrata Pdr1 regulon. *Eukaryot. Cell* **10**, 373–383 (2010).
37. Paul, S., Schmidt, J. A. & Scott Moye-Rowley, W. Regulation of the CgPdr1 transcription factor from the pathogen candida glabrata. *Eukaryot. Cell* **10**, 187–197 (2011).
38. Vermitsky, J. P. *et al.* Pdr1 regulates multidrug resistance in Candida glabrata: Gene disruption and genome-wide expression studies. *Mol. Microbiol.* **61**, 704–722 (2006).
39. Nobile, C. J. *et al.* A Recently Evolved Transcriptional Network Controls Biofilm Development in Candida albicans. *NHI* **148**, 126–138 (2012).
40. Invergo, B., Ames, R. & Usher, J. Data-driven prediction of genetic interactions in Candida glabrata. *Access Microbiol.* **1**, 8 (2019).
41. Typas, A. *et al.* A tool-kit for high-throughput, quantitative analyses of genetic interactions in E. coli HHS Public Access. *Nat Methods* **5**, 781–787 (2008).
42. Batzoglou, S., Myers, R. M. & Sidow, A. Genome-Wide Analysis of Transcription Factor Binding Sites Based on ChIP-Seq Data. *Nat. Methods* **5**, 829–834 (2010).
43. S.cerevisiae - Yeastract. Available at: http://yeastract-plus.org/yeastract/scerevisiae/view.php?existing=protein&proteinname=Hap1p. (Accessed: 6th July 2020)
44. C.albicans - PathoYeastract. Available at: http://yeastract-plus.org/pathoyeastract/calbicans/view.php?existing=locus&orfname=C2_06470W_A. (Accessed: 6th July 2020)